EAI Endorsed Transactions
on Industrial Networks and Intelligent Systems
Research Article **EAI.EU**

Security-Reliability Analysis of NOMA-Assisted Hybrid Satellite-Terrestrial Relay Multi-Cast Transmission Networks Using Fountain Codes and Partial Relay Selection with Presence of Multiple Eavesdroppers

Nguyen Van Toan[1], Tran Trung Duy[2,*], Pham Ngoc Son[1], Pham Viet Tuan[3], Lam-Thanh Tu[4]

[1]Ho Chi Minh City University of Technology and Education, Ho Chi Minh City, VietNam
[2]Posts and Telecommunications Institute of Technology, HaNoi, Vietnam
[3]University of Education, Hue University, Hue City, Vietnam
[4]Communication and Signal Processing Research Group, Faculty of Electrical and Electronics Engineering, Ton Duc Thang University, Ho Chi Minh City, Vietnam

Abstract

This article proposes a hybrid satellite-terrestrial relaying network (HSTRN) that integrates physical-layer security (PLS), Fountain codes (FCs), non-orthogonal multiple access (NOMA), and partial relay selection (PRS) to enhance system performance in terms of reliability, data rate, and security. In the proposed system, a satellite uses NOMA to simultaneously transmit Fountain packets to two clusters of terrestrial users. Data transmission is assisted by one of the terrestrial relay stations, selected by the PRS algorithm. We derive exact expressions for outage probability (OP) and system outage probability (SOP) at the legitimate users, as well as intercept probability (IP) and system intercept probability (SIP) at eavesdroppers. Monte Carlo simulations are realized to validate the accuracy of the analytical results, illustrate performance trends, and analyse the impact of key parameters on the considered performance.

Received on 04 February 2025; accepted on 30 March 2025; published on 11 April 2025

Keywords: *Hybrid satellite-terrestrial relaying networks*, *Fountain codes*, *non-orthogonal multiple access*, *physical-layer security*, *multicast transmission*, *Fountain codes*

doi:10.4108/eetinis.v12i3.8604

1. Introduction

This paper studies Hybrid Satellite-Terrestrial Relay Networks (HSTRNs) [1–3], where ground relay stations are deployed to assist the data communication between satellites and terrestrial users. As a result, HSTRNs enhance signal quality, expand network coverage, and ensure stable and reliable connections in fading environments. HSTRNs are expected to serve as a foundation for 5G/B5G networks, meeting the demands of fast connectivity and low latency.

Recently, Non-Orthogonal Multiple Access (NOMA) [4–7] has been applied into HSTRNs to enhance the system's data rate. In [8], a satellite employs NOMA to serve multiple multi-antenna ground users via help of a terrestrial station using amplify-and-forward (AF) technique. In addition, a power allocation strategy is applied to the signals transmitted by the satellite, while a successive interference cancellation (SIC) technique is implemented at the users. The authors in [8] also derived exact and asymptotic expressions of outage probability (OP) for the proposed scheme to evaluate the system diversity and coding gain. In [9], the authors studied performance of the NOMA – HSTRN scheme, where the AF or Decode-and-Forward (DF)

*Corresponding author. Email: trantrungduy@ptithcm.edu.vn

technique was used by a terrestrial station. In [9], the OP performance and fairness among users, under the condition of imperfect channel state information, was also analyzed. In [10], the authors considered the case where some ground users can directly connect to the satellite, while others can only receive data via multi-antenna DF terrestrial stations. Published works [11, 12] proposed the models, respectively operating in underlay and overlay cognitive radio environments. In [11, 12], the satellites and terrestrial stations function as secondary devices that must adaptively adjust their operations to ensure the quality of service for primary networks.

Recently, physical-layer security (PLS) [13–16] has been incorporated into HSTRNs to enhance information security. In PLS secure communication can be achieved by leveraging the characteristics of wireless channels, such as the distances and channel conditions between nodes. In [17], the authors introduced a threshold-based scheduling method to improve security by analyzing secrecy outage probability in HSTRNs with multiple ground users and eavesdroppers. In addition, both colluding and non-colluding passive eavesdropping schemes are studied in [17]. The authors of [18] proposed a joint relay selection and user scheduling strategy to enhance the OP performance of PLS – HSTRNs with presence of the colluding and non-colluding eavesdroppers. Published work [19] proposed a reconfigurable intelligent surface (RIS)-aided HSTRNs scenario. Unlike conventional relaying techniques that use cooperative relays, the RIS-aided relaying schemes employ intelligent surfaces to optimally reflect incoming signals to the intended users [20–22]. In [23], the authors analyzed secrecy performance of PLS – HSTRNs for both single-relay and multi-relay selection scenarios. In particular, the single-relay scheme selects the successful relay with the highest channel capacity of the relay-destination links, while the multi-relay scheme allows all successful relays to participate in data transmission at the cooperative phase. A security-reliability tradeoff (SRT) in PLS – HSTRNs was investigated in [24], where the secrecy performance was evaluated via intercept probability (IP) at the eavesdroppers and OP at the legitimate users. In addition, the authors in [24] proposed a relay selection model to enhance the performance under impact of co-channel interference.

Fountain codes (FCs) [25–27] have proven to be an effective technique in wireless communication networks due to their simple implementation and adaptability to environmental changes. Moreover, FCs also enable secure communication if the legitimate users can obtain enough encoded packets while the eavesdroppers cannot. In the context of HSTRNs utilizing FCs, until now, there have been only several reports such as [28–31]. In [28], the authors evaluated outage performance of utilizing FCs in co-channel interference environment. The authors of [29] studied the SRT performance for PLS – HSTRNs using FCs and cooperative jamming technique, where a jammer node was employed to send noises to a passive eavesdropper. In [30], both NOMA and RIS techniques were applied into FCs - aided PLS – HSTRNs to enhance the SRT performance, in presence of multiple eavesdroppers. Published work [31] studied the OP performance of HSTRNs with two groups of ground users and using FCs and NOMA.

This paper proposes the PLS – HSTRNs scheme that combines FC and NOMA to improve system performance in reliability, data rate, and security. In particular, a satellite uses NOMA to deliver two Fountain packets to two clusters of terrestrial users simultaneously. Each data transmission from the satellite to the users occurs in two time slots, and is assisted by one of terrestrial relay stations. In addition, partial relay selection (PRS) algorithm [32, 33] is applied to select the terrestrial relay station.

Different from the previous works related to performance evaluation of HSTRNs using PLS and/or NOMA [1–3], [8–12], [17–24], in this paper, we apply FCs into the proposed system model. Unlike [28–31], the PRS algorithm is employed to enhance the reliable communication between the satellite-terrestrial links. Moreover, we also consider a generalized system model with multi-cast transmission scheme under the presence of multiple eavesdroppers.

The main contribution of this paper can be outlined as follows. We first derive exact closed-form expressions of OP and system outage probability (SOP) at the legitimate users, as well as IP and system intercept probability (IP) at the eavesdroppers. Next, we realize computer simulations to verify the derived expressions of OP, IP, SOP and SIP. Finally, we investigate the impact of key system parameters on the OP, IP, SOP and SIP performance, and the SRT performance is evaluated.

The rest of the paper is organized as follows. Section 2 describes the proposed system model. Section 3 presents performance analysis. Simulation results are given in Section 4. Finally, Section 5 concludes the paper.

2. System Model

Fig. 1 presents the proposed PLS-HSTRN, where the satellite (S) wants to transmit data to two clusters of ground users. Let m_1 and m_2 denote the desired data of the users in clusters 1 and 2, respectively. Due to severe obstruction and shadowing effects, the signals transmitted from S cannot directly reach the clusters, which is a widely accepted assumption in HSTRN studies [34, 35]. To assist the satellite-ground user transmission, K terrestrial stations are deployed,

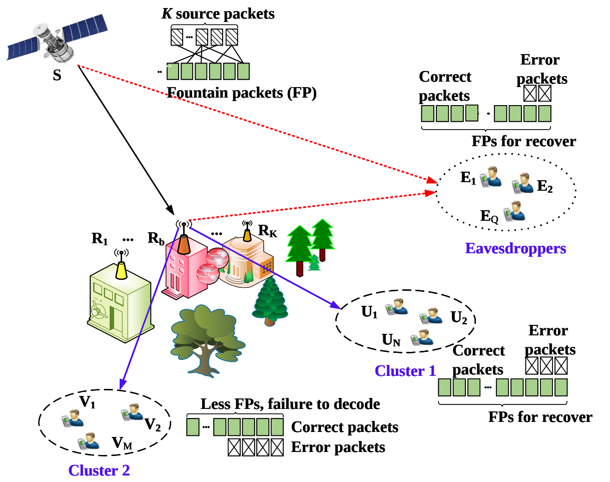

Figure 1. The proposed HSTRN scheme using PLS, FCs and NOMA.

and they are denoted by $\mathrm{R}_1, \mathrm{R}_2, \ldots, \mathrm{R}_K$. In addition, one of these stations (denoted by R_b) is selected using the PRS technique. Let N and M denote the number of members in clusters 1 and 2. Then, the ground users in clusters 1 and 2 are denoted by $\{\mathrm{U}_1, \mathrm{U}_2, \ldots, \mathrm{U}_N\}$ and $\{\mathrm{V}_1, \mathrm{V}_2, \ldots, \mathrm{V}_M\}$, respectively. We consider the multi-eavesdropper scheme, where Q eavesdroppers $(\mathrm{E}_1, \mathrm{E}_2, \ldots, \mathrm{E}_Q)$ attempt to illegally decode m_1 and m_2. We assume that these eavesdroppers can directly receive the data from the satellite and are located close to each other. It is also assumed that all the nodes $(\mathrm{S}, \mathrm{R}_k, \mathrm{U}_n, \mathrm{V}_m, \mathrm{E}_q)$ are single-antenna, half-duplex devices, where $k = 1, \ldots, K$; $n = 1, \ldots, N$; $m = 1, \ldots, M$, and $q = 1, \ldots, Q$.

Using FCs, S can create Fountain packets from m_1 and m_2, denoted by p_1 and p_2, respectively. Then, S uses NOMA to transmit both p_1 and p_2 to R_b in the first time slot. If R_b successfully decodes both p_1 and p_2, it also employs NOMA to send both p_1 and p_2 to the users in the clusters 1 and 2 at the second time slot. If R only decodes p_2 correctly, it will only send p_2 to the cluster 2 at the second time slot. All the eavesdroppers can receive p_1 and p_2 from S and R_b in two time slots. Due to the delay constraint, the maximum number of data transmissions by S is limited by $H_{\max}$. In addition, the minimum number of packets required for the successful recovery of m_1 and m_2 is $G_{\min}$, where $G_{\min} \leq H_{\max}$.

Let g_{XY} denote the channel gain of the X–Y link, where $X, Y \in \{\mathrm{S}, \mathrm{R}_k, \mathrm{U}_n, \mathrm{V}_m, \mathrm{E}_q\}$. Considering the S–$Z$ links, the channel gain $g_{\mathrm{S}Z}$ has the following Probability Density Function (PDF) as (see [30, 31]):

$$f_{g_{\mathrm{S}Z}}(x) = \frac{1}{2b_{\mathrm{ST}}}\left(\frac{2a_{\mathrm{ST}}b_{\mathrm{ST}}}{2a_{\mathrm{ST}}b_{\mathrm{ST}} + \Omega_{\mathrm{ST}}}\right)^{a_{\mathrm{ST}}} exp\left(-\frac{x}{2b_{\mathrm{ST}}}\right) \times {}_1F_1\left(a_{\mathrm{ST}}; 1; \frac{\Omega_{\mathrm{ST}}x}{2b_{\mathrm{ST}}(2a_{\mathrm{ST}}b_{\mathrm{ST}} + \Omega_{\mathrm{ST}})}\right), \quad (1)$$

where $Z \in \{\mathrm{R}_k, \mathrm{E}_q\}$, $T \in \{\mathrm{R}, \mathrm{E}\}$, $2b_{ST}$ and Ω_{ST} are powers of multi-path and line of sight components, respectively, a_{ST} is the channel parameter, and ${}_1F_1(.;.;.)$ is the confluent hypergeometric function of the first kind [30, 31].

It is worth noting from (1) that this paper considers a block fading channel, and the g_{XY} values are identically and independently distributed (i.i.d.) random variables (RVs), i.e., $\omega_{\mathrm{SR}_k} = \omega_{\mathrm{SR}}$ and $\omega_{\mathrm{SE}_q} = \omega_{\mathrm{SE}}$, for $\forall k, q$, and $\forall \omega \in \Omega = \{a, b, \Omega\}$.

From (1), Cumulative Distribution Function (CDF) of $g_{\mathrm{S}Z}$ can be expressed as (see[29, 36]):

$$F_{g_{\mathrm{S}Z}}(x) = 1 - \alpha_{\mathrm{ST}}^{a_{\mathrm{ST}}}\psi_{\mathrm{ST}}\sum_{n_{\mathrm{ST}}=0}^{a_{\mathrm{ST}}-1}\xi_{\mathrm{ST}}(n_{\mathrm{ST}}) \times \sum_{q_{\mathrm{ST}}=0}^{n_{\mathrm{ST}}}\frac{n_{\mathrm{ST}}!\,x^{q_{\mathrm{ST}}}e^{-(\psi_{\mathrm{ST}}-\beta_{\mathrm{ST}})x}}{q_{\mathrm{ST}}!(\psi_{\mathrm{ST}} - \beta_{\mathrm{ST}})^{n_{\mathrm{ST}}-q_{\mathrm{ST}}+1}}, \quad (2)$$

where $\psi_{\mathrm{ST}} = 1/2b_{\mathrm{ST}}$,

$$\xi_{\mathrm{ST}}(n_{\mathrm{ST}}) = \frac{(-1)^{n_{\mathrm{ST}}}(1 - a_{\mathrm{ST}})_{n_{\mathrm{ST}}}\beta_{\mathrm{ST}}^{n_{\mathrm{ST}}}}{n_{\mathrm{ST}}!}$$
$$\alpha_{\mathrm{ST}} = \left(\frac{2a_{\mathrm{ST}}b_{\mathrm{ST}}}{2a_{\mathrm{ST}}b_{\mathrm{ST}} + \Omega_{\mathrm{ST}}}\right)^{a_{\mathrm{ST}}},$$
$$\beta_{\mathrm{ST}} = \frac{\Omega_{\mathrm{ST}}}{2b_{\mathrm{ST}}(2a_{\mathrm{ST}}b_{\mathrm{ST}} + \Omega_{\mathrm{ST}})}, \quad (3)$$

and $(.)_{n_{\mathrm{ST}}}$ is the Pochhammer symbol [36].

For the terrestrial links, the channel gain $g_{\mathrm{R}_k W}$ has the following probability density function (PDF) and cumulative distribution function (CDF), respectively, as given in [37–39]:

$$f_{g_{\mathrm{R}_k\mathrm{W}}}(x) = \lambda_{\mathrm{R}_k\mathrm{W}}\exp(-\lambda_{\mathrm{R}_k\mathrm{W}}x),$$
$$F_{g_{\mathrm{R}_k\mathrm{W}}}(x) = 1 - \exp(-\lambda_{\mathrm{R}_k\mathrm{W}}x), \quad (4)$$

where $\mathrm{W} \in \left\{\mathrm{U}_n, \mathrm{V}_m, \mathrm{E}_q\right\}$.

It is worth noting that the assumption that nodes within a cluster receive the same data is made for ease of presentation and analysis. In addition, it is also assumed that the users within the same cluster have approximately equal distances (see [40]), we have $\lambda_{\mathrm{R}_k\mathrm{W}} = \lambda_{\mathrm{R}_k\mathrm{B}}$, where $\mathrm{B} \in \{\mathrm{U}, \mathrm{V}, \mathrm{E}\}$. Here, U, V, and E are denoted as the nodes in Cluster 1, Cluster 2, and the group of eavesdroppers, respectively. In (4), $\lambda_{\mathrm{R}_k\mathrm{B}}$ denotes a parameter of $g_{\mathrm{R}_k\mathrm{B}}$ [37].

Next, the PRS algorithm can be given, similar to [32, 33], as

$$\mathrm{R}_b : g_{\mathrm{SR}_b} = \max_{k=1,2,\ldots,K} \left(g_{\mathrm{SR}_k} \right). \tag{5}$$

Equation (5) implies that the station is selected to provide the highest instantaneous channel for the satellite-terrestrial station links. Due to the assumption of i.i.d. random variables (RVs), CDF of g_{SR_b} can be given as

$$F_{g_{\mathrm{SR}_b}}(x) = \Pr\left(\max_{k=1,2,\ldots,K} g_{\mathrm{SR}_k} < x \right) = \left[F_{g_{\mathrm{SR}_k}}(x) \right]^K. \tag{6}$$

Now, we consider the data transmission at two time slots. At the first one, S first combines the modulated signals of symbols in p_1 and p_2 as (see [4–7]):

$$s_{\mathrm{S}}[l] = \sqrt{\alpha_1 P_{\mathrm{S}}}\, s_{p_1}[l] + \sqrt{\alpha_2 P_{\mathrm{S}}}\, s_{p_2}[l], \tag{7}$$

where $l = 1, 2, \ldots, L$, and L is the number of symbols in p_1 and p_2. Here, $s_{p_1}[l]$ and $s_{p_2}[l]$ are the lth modulated signals correspond to the lth symbols in p_1 and p_2, respectively. P_{S} is the transmit power of S, and α_1 and α_2 are power allocation factors, i.e., $\alpha_1 + \alpha_2 = 1$ and $0 < \alpha_1, \alpha_2 < 1$.

To clearly illustrate the operation at the selected relay station and the eavesdroppers, we provide Table 1, which summarizes all possible cases of the decoding status at these nodes (see the top of the next page).

In this paper, we assume that the power allocation factors α_1 and α_2 are the same in two time slots [30, 31]. Then, S sends s_{S} to R_b, while E_q also attempts to overhear s_{S}. Then, the node $\mathrm{Y} \in \{\mathrm{R}_b, \mathrm{E}_q\}$ performs successive interference cancellation (SIC) to decode p_2 and p_1 in turn. Similar to [30, 31], the Signal-to-Noise Ratios (SNRs) obtained at Y for decoding p_2 and p_1 can be expressed, respectively, as

$$\gamma_{\mathrm{SY,p_2}} = \frac{\alpha_2 P_{\mathrm{S}} g_{\mathrm{SY}}}{\alpha_1 P_{\mathrm{S}} g_{\mathrm{SY}} + \sigma_0^2}, \quad \gamma_{\mathrm{SY,p_1}} = \frac{\alpha_1 P_{\mathrm{S}} g_{\mathrm{SY}}}{\sigma_0^2}, \tag{8}$$

where σ_0^2 is the variance of Gaussian noise.

At the second time slot, if R_b can decode both p_1 and p_2 correctly from S (CASE 1), R_b also combines the modulated signals of symbols in p_1 and p_2 as

$$s_{\mathrm{R}}[l] = \sqrt{\alpha_1 P_{\mathrm{R}}}\, s_{p_1}[l] + \sqrt{\alpha_2 P_{\mathrm{SR}}}\, s_{p_2}[l], \tag{9}$$

where P_{R} is the transmit power of R_b. Next, R_b broadcasts s_{R} to two clusters.

Considering the user V_m of cluster 2, it directly decodes p_2, with the obtained SNR as

$$\gamma_{\mathrm{R}_b\mathrm{V}_m,p_2} = \frac{\alpha_2 P_{\mathrm{R}} g_{\mathrm{R}_b\mathrm{V}_m}}{\alpha_1 P_{\mathrm{R}} g_{\mathrm{R}_b\mathrm{V}_m} + \sigma_0^2}. \tag{10}$$

For the user U_n of cluster 1, it must decode p_2 and then use SIC to decode p_1. The obtained SNRs, with respect to p_2 and p_1, can be given, respectively, as

$$\gamma_{\mathrm{R}_b\mathrm{U}_n,p_2} = \frac{\alpha_2 P_{\mathrm{R}} g_{\mathrm{R}_b\mathrm{U}_n}}{\alpha_1 P_{\mathrm{R}} g_{\mathrm{R}_b\mathrm{U}_n} + \sigma_0^2}, \gamma_{\mathrm{R}_b\mathrm{U}_n,p_1} = \frac{\alpha_1 P_{\mathrm{R}} g_{\mathrm{R}_b\mathrm{U}_n}}{\sigma_0^2}. \tag{11}$$

Similarly, E_q also performs SIC to decode p_2 and p_1 in the second time slot. Then, the obtained SNRs, with respect to p_2 and p_1, can be formulated, respectively, as

$$\gamma_{\mathrm{R}_b\mathrm{E}_q,p_2} = \frac{\alpha_2 P_{\mathrm{R}} g_{\mathrm{R}_b\mathrm{E}_q}}{\alpha_1 P_{\mathrm{R}} g_{\mathrm{R}_b\mathrm{E}_q} + \sigma_0^2}, \gamma_{\mathrm{R}_b\mathrm{E}_q,p_1} = \frac{\alpha_1 P_{\mathrm{R}} g_{\mathrm{R}_b\mathrm{E}_q}}{\sigma_0^2}. \tag{12}$$

Here, if E_q correctly decodes both p_2 and p_1 in the first time slot, it will do nothing in the second time slot.

Next, considering the case where R_b correctly decodes p_2 and incorrectly decodes p_1 (CASE 2); then, R_b only sends p_2 to cluster 2 with the transmit power P_{R}. Therefore, the SNR at V_m is $\varphi_{\mathrm{R}_b\mathrm{V}_m,p_2} = \frac{P_{\mathrm{R}} g_{\mathrm{R}_b\mathrm{V}_m}}{\sigma_0^2}$. For E_q, if it cannot correctly decode p_2 from S, it will decode p_2, with the SNR is $\varphi_{\mathrm{R}_b\mathrm{E}_q,p_2} = \frac{P_{\mathrm{R}} g_{\mathrm{R}_b\mathrm{E}_q}}{\sigma_0^2}$.

3. Performance Analysis

We first assume that the receiver Y can correctly decode one Fountain packet from the transmitter X if the SNR γ_{XY} is higher than a threshold (denoted by γ_{th}). Conversely, if $\gamma_{XY} \le \gamma_{\mathrm{th}}$, then the decoding at Y fails. From (2), (6), and (8), we calculate the probability that R_b correctly decodes both p_2 and p_1 from S as

$$\begin{aligned}
\theta_{\mathrm{R}_b,p_2,p_1} &= \Pr\left(\gamma_{\mathrm{SR}_b,p_2} > \gamma_{\mathrm{th}}, \gamma_{\mathrm{SR}_b,p_1} > \gamma_{\mathrm{th}} \right) \\
&= 1 - F_{g_{\mathrm{SR}_b}}(\rho_{\max}) \\
&= 1 - \left[\begin{array}{c} 1 - \alpha_{\mathrm{SR}}^{a_{\mathrm{SR}}} \psi_{\mathrm{SR}} \sum\limits_{n_{\mathrm{SR}}=0}^{a_{\mathrm{SR}}-1} \xi_{\mathrm{SR}}(n_{\mathrm{SR}}) \\ \times \sum\limits_{q_{\mathrm{SR}}=0}^{n_{\mathrm{SR}}} \frac{n_{\mathrm{SR}}!\rho_{\max}^{q_{\mathrm{SR}}} e^{-(\psi_{\mathrm{SR}}-\beta_{\mathrm{SR}})\rho_{\max}}}{q_{\mathrm{SR}}!(\psi_{\mathrm{SR}}-\beta_{\mathrm{SR}})^{n_{\mathrm{SR}}-q_{\mathrm{SR}}+1}} \end{array} \right]^K.
\end{aligned} \tag{13}$$

In (13), α_2 and α_1 satisfy the condition $\alpha_2 > \alpha_1 \gamma_{\mathrm{th}}$ [30, 31], $\Lambda = \frac{P_{\mathrm{S}}}{\sigma_0^2}$, and

$$\begin{aligned}
\rho_{\mathrm{th},1} &= \frac{\gamma_{\mathrm{th}}}{\Lambda(\alpha_2 - \alpha_1 \gamma_{\mathrm{th}})}, \rho_{\mathrm{th},2} = \frac{\gamma_{\mathrm{th}}}{\Lambda \alpha_1}, \\
\rho_{\max} &= \max\left(\rho_{\mathrm{th},1}, \rho_{\mathrm{th},2} \right).
\end{aligned} \tag{14}$$

Next, we calculate the probability that R_b correctly decodes p_2 and incorrectly decodes p_1 as

$$\begin{aligned}
\theta_{\mathrm{R}_b,p_2,\overline{p_1}} &= \Pr\left(\gamma_{\mathrm{SR}_b,p_2} > \gamma_{\mathrm{th}}, \gamma_{\mathrm{SR}_b,p_1} \le \gamma_{\mathrm{th}} \right) \\
&= F_{g_{\mathrm{SR}_b}}\left(\rho_{\mathrm{th},2} \right) - F_{g_{\mathrm{SR}_b}}\left(\rho_{\mathrm{th},1} \right),
\end{aligned} \tag{15}$$

where $\rho_{\mathrm{th},2} > \rho_{\mathrm{th},1}$ or $\alpha_2 > \alpha_1(1 + \gamma_{\mathrm{th}})$. Substituting (2) and (6) into (15), we obtain an exact expression of $\theta_{\mathrm{R}_b,p_2,\overline{p_1}}$.

Table 1. Decoding status at R_b and E_q in two time slots

Receiver	First time slot	Second time slot
R_b	**Case 1:** R_b successfully decodes both p_2 and p_1 from S	R_b re-encodes and forwards p_2 and p_1 to two clusters
	Case 2: R_b successfully decodes p_2 but fails to decode p_1 from S	R_b re-encodes and forwards p_2 to cluster 2
E_q	**Case 3.1:** E_q successfully decodes both p_2 and p_1 from S	Not decode p_2 and p_1 any more
	Case 3.2: E_q successfully decodes p_2 but fails to decode p_1 from S	E_q applies SIC, removes p_2, and decodes p_1 from R_b
	Case 3.3: E_q correctly decodes p_2 from S (not considering the decoding of p_1)	Not decode p_2 any more

Similarly, based on Table 1, the probabilities that E_q follows Case 3.1, Case 3.2, and Case 3.3 are, respectively, given by:

$$\begin{aligned}\mu_{\mathrm{E}_q,p_2,p_1} &= \Pr\left(\gamma_{\mathrm{SE}_q,p_2} > \gamma_{\mathrm{th}}, \gamma_{\mathrm{SE}_q,p_1} > \gamma_{\mathrm{th}}\right) \\ &= 1 - F_{g_{\mathrm{SE}_q}}(\rho_{\max}), \end{aligned} \tag{16}$$

$$\begin{aligned}\mu_{\mathrm{E}_q,p_2,\overline{p_1}} &= \Pr\left(\gamma_{\mathrm{SE}_q,p_2} > \gamma_{\mathrm{th}}, \gamma_{\mathrm{SE}_q,p_1} \le \gamma_{\mathrm{th}}\right) \\ &= F_{g_{\mathrm{SE}_q}}(\rho_{\mathrm{th},2}) - F_{g_{\mathrm{SE}_q}}(\rho_{\mathrm{th},1}), \end{aligned} \tag{17}$$

$$\mu_{\mathrm{E}_q,p_2} = \Pr\left(\gamma_{\mathrm{SE}_q,p_2} > \gamma_{\mathrm{th}}\right) = 1 - F_{g_{\mathrm{SE}_q}}(\rho_{\mathrm{th},1}). \tag{18}$$

Now, we consider the data transmission at the second time slot. In CASE 1, R_b uses NOMA to send both p_2 and p_1 to two clusters; from (4) and (10), the probability that V_m correctly decodes p_2 is calculated as

$$\chi_{\mathrm{V},p_2} = \Pr\left(\gamma_{\mathrm{R}_b\mathrm{V}_m,p_2} > \gamma_{\mathrm{th}}\right) = \exp\left(-\lambda_{\mathrm{RV}}\omega_{1,\mathrm{th}}\right), \tag{19}$$

where $\omega_{1,\mathrm{th}} = \frac{\sigma_0^2\gamma_{\mathrm{th}}}{(\alpha_2-\alpha_1\gamma_{\mathrm{th}})P_{\mathrm{R}}}$.

For U_n, the probability that it correctly decodes p_1 (it must correctly decode p_2 first) is given as

$$\begin{aligned}\chi_{\mathrm{U},p_1} &= \Pr\left(\gamma_{\mathrm{R}_b\mathrm{U}_n,p_2} > \gamma_{\mathrm{th}}, \gamma_{\mathrm{R}_b\mathrm{U}_n,p_1} > \gamma_{\mathrm{th}}\right) \\ &= \exp\left(-\lambda_{\mathrm{RV}}\omega_{\max}\right), \end{aligned} \tag{20}$$

where $\omega_{2,\mathrm{th}} = \frac{\sigma_0^2\gamma_{\mathrm{th}}}{\alpha_2 P_{\mathrm{R}}}$, $\omega_{\max} = \max\left(\omega_{1,\mathrm{th}}, \omega_{2,\mathrm{th}}\right)$.

Assume that E_q cannot obtain both p_2 and p_1 at the first time slot. Then, the probability of successfully decoding p_2 at E_q in CASE 1 is calculated as

$$\chi_{\mathrm{E},p_2} = \Pr\left(\gamma_{\mathrm{R}_b\mathrm{E}_q,p_2} > \gamma_{\mathrm{th}}\right) = \exp\left(-\lambda_{\mathrm{RE}}\omega_{1,\mathrm{th}}\right), \tag{21}$$

and the probability of successfully decoding p_1 at E_q in CASE 1 (it must correctly decode p_2 first) is given as

$$\begin{aligned}\chi_{\mathrm{E},p_2,p_1} &= \Pr\left(\gamma_{\mathrm{R}_b\mathrm{E}_q,p_2} > \gamma_{\mathrm{th}}, \gamma_{\mathrm{R}_b\mathrm{E}_q,p_1} > \gamma_{\mathrm{th}}\right) \\ &= \exp\left(-\lambda_{\mathrm{RE}}\omega_{\max}\right). \end{aligned} \tag{22}$$

In CASE 3.1 and CASE 3.2, E_q does not need to decode p_2 from R_b anymore. Instead, it uses SIC to remove p_2 from the received signal and then decodes p_1. Hence, the probability of successfully decoding p_1 at E_q in these cases is computed as

$$\chi_{\mathrm{E},p_1} = \Pr\left(\gamma_{\mathrm{R}_b\mathrm{E}_q,p_1} > \gamma_{\mathrm{th}}\right) = \exp\left(-\lambda_{\mathrm{RE}}\omega_{2,\mathrm{th}}\right). \tag{23}$$

For CASE 2, the probability of correctly decoding p_2 at V_m is computed as

$$\tau_{\mathrm{V},p_2} = \Pr(\varphi_{\mathrm{R}_b\mathrm{V}_m,p_2} > \gamma_{\mathrm{th}}) = \exp(-\lambda_{\mathrm{RV}}\omega_{3,\mathrm{th}}), \tag{24}$$

where $\omega_{3,\mathrm{th}} = \frac{\sigma_0^2\gamma_{\mathrm{th}}}{P_{\mathrm{R}}}$.

If E_q cannot obtain p_2 at the first time slot, then, the probability of correctly decoding p_2 at E_q is given as

$$\tau_{\mathrm{E},p_2} = \Pr\left(\varphi_{\mathrm{R}_b\mathrm{E}_q,p_2} > \gamma_{\mathrm{th}}\right) = \exp\left(-\lambda_{\mathrm{RE}}\omega_{3,\mathrm{th}}\right). \tag{25}$$

3.1. OP and SOP

The decoding of m_2 and m_1 at V_m (U_n) is successful if V_m (U_n) can collect at least $G_{\min}$ Fountain packets. Otherwise, the decoding at V_m (U_n) is in outage.

For Cluster 1, the probability that all the nodes in this cluster correctly recover m_1 is calculated as

$$\begin{aligned}\overline{\mathrm{OP}_1} = &\sum_{r=G_{\min}}^{H_{\max}} C_{H_{\max}}^r (\theta_{\mathrm{R_b},p_2,p_1})^r (1-\theta_{\mathrm{R_b},p_2,p_1})^{H_{\max}-r} \\ &\times\left[\sum_{l=G_{\min}}^{r} C_r^l \chi_{\mathrm{U},p_1}^l (1-\chi_{\mathrm{U},p_1})^{r-l}\right]^N, \end{aligned} \tag{26}$$

where C_b^a ($b \ge a$) denotes a binomial coefficient, i.e., $C_b^a = \frac{b!}{a!(b-a)!}$, r denotes the number of times that R_b correctly decodes both p_2 and p_1, and l is the number of times that U_n correctly decodes p_1 at the second time slot. It is worth noting from (26) that there are $C_{H_{\max}}^r$ cases where the selected relay station correctly receives both p_2 and p_1, r times. Moreover, for all the nodes in the Cluster 1 to correctly obtain at least G_{min} packets p_1, we must have $r \geq G_{\min}$ and $r \geq l \geq G_{\min}$. Finally, $(1-\theta_{\mathrm{R}_b,p_2,p_1})$ is the probability that R_b cannot decode p_1 correctly at the first time slot, and $(1-\chi_{\mathrm{U},p_1})$ is the probability that U_n $(\forall n = 1, 2, \ldots, N)$ cannot decode p_1 correctly at the second time slot.

Equation (26) shows that $\overline{\mathrm{OP}_1}$ is impacted by the FCs parameters H_{max} and G_{min}. Moreover, $\overline{\mathrm{OP}_1}$ is directly proportional to the number of users in cluster 1. These observations will be verified in Section 4.

Substituting (13) and (20) into (26), we obtain an exact closed-form expression of $\overline{\mathrm{OP}_1}$.

Considering Cluster 2, we first denote t_{tot} as the number of times that R_b correctly decodes p_2 at the first time slot, where $G_{\min} \leq t_{\mathrm{tot}} \leq H_{\max}$. Let t_1 as the number of times that R_b correctly receives both p_2 and p_1 (CASE 1). Then, $t_2 = t_{\mathrm{tot}} - t_1$ is the number of times that R_b only correctly receives p_2 (not p_1) (CASE 2). Next, let r_1 and r_2 denote the number of times of the successful decoding of p_2 at V_m in CASE 1 and CASE 2, respectively, where $r_1 \leq t_1$ and $r_2 \leq t_2$. If $r_1 + r_2 \geq G_{\min}$, then V_m can correctly recover the desired data m_2. Next, we can calculate the probability that all the nodes of Cluster 2 can correctly recover m_2 as follows:

$$
\begin{aligned}
&\overline{\mathrm{OP}_2} = \sum_{t_{\mathrm{tot}}=G_{\min}}^{H_{\max}} \sum_{t_1=0}^{t_{\mathrm{tot}}} C_{H_{\max}}^{t_1} C_{H_{\max}-t_1}^{t_{\mathrm{tot}}-t_1} (\theta_{\mathrm{R_b},p_2,p_1})^{t_1} (\theta_{\mathrm{R}_b,p_2,\overline{p_1}})^{t_{\mathrm{tot}}-t_1} \\
&\times (1-\theta_{\mathrm{R_b},p_2,p_1} - \theta_{\mathrm{R}_b,p_2,\overline{p_1}})^{H_{\max}-t_{\mathrm{tot}}} \\
&\times \left[\sum_{r_1=0}^{t_1} \sum_{\substack{r_2=0,\\ r_1+r_2\geq G_{\min}}}^{t_{\mathrm{tot}}-t_1} \begin{array}{l} C_{t_1}^{r_1} C_{t_{\mathrm{tot}}-t_1}^{r_2} (\chi_{\mathrm{V},p_2})^{r_1} (1-\chi_{\mathrm{V},p_2})^{t_1-r_1} \\ \times \tau_{\mathrm{V},p_2}^{r_2} (1-\tau_{\mathrm{V},p_2})^{t_{\mathrm{tot}}-t_1-r_2} \end{array} \right]^M .
\end{aligned} \tag{27}
$$

Substituting (13), (15), (19), and (24) into (27), we obtain an exact closed-form expression of $\overline{\mathrm{OP}_2}$.

In (27), $(1-\theta_{\mathrm{R_b},p_2,p_1} - \theta_{\mathrm{R}_b,p_2,\overline{p_1}})$ is the probability that R_b cannot decode p_2 and p_1 correctly at the first time slot, $(1-\chi_{\mathrm{V},p_2})$ and $(1-\tau_{\mathrm{V},p_2})$ are the probabilities that V_m $(\forall m = 1, 2, \ldots, M)$ cannot correctly decode p_2 in CASE 1 and CASE 2, respectively. The factors affecting $\overline{\mathrm{OP}_2}$ include FC parameters, the probability of successfully decoding a single packet p_2, and the number of users in cluster 2.

Next, we define the OP of Cluster i as the probability that at least one of the users in this cluster is outage, where $i \in \{1, 2\}$. Using (26) and (27), we obtain exact closed-form expressions of OP for Clusters 1 and 2, respectively, as follows:

$$
\mathrm{OP}_1 = 1 - \overline{\mathrm{OP}_1}, \mathrm{OP}_2 = 1 - \overline{\mathrm{OP}_2}. \tag{28}
$$

Finally, the SOP is defined as the probability that Cluster 1 or Cluster 2 is outage, and it is computed as:

$$
\mathrm{SOP}_1 = 1 - \overline{\mathrm{OP}_1} \times \overline{\mathrm{OP}_2}. \tag{29}
$$

3.2. IP and SIP

For E_q, it attempts to collect at least $G_{\min}$ packets p_2 and $G_{\min}$ packets p_1 to recover the data m_2 and m_1, respectively. At first, the probability that E_q correctly decodes one packet p_2 can be formulated as:

$$
\begin{aligned}
\Lambda_{\mathrm{E}_q,p_2} &= \Pr\left(\gamma_{\mathrm{SE}_q,p_2} > \gamma_{\mathrm{th}}\right) + \Pr\left(\gamma_{\mathrm{SE}_q,p_2} \leq \gamma_{\mathrm{th}}\right) \\
&\times \left[\begin{array}{l} \Pr\left(\gamma_{\mathrm{SR_b},p_2} > \gamma_{\mathrm{th}}, \gamma_{\mathrm{SR_b},p_1} > \gamma_{\mathrm{th}}\right) \Pr\left(\gamma_{\mathrm{R}_b\mathrm{E}_q,p_2} > \gamma_{\mathrm{th}}\right) \\ + \Pr\left(\gamma_{\mathrm{SR_b},p_2} > \gamma_{\mathrm{th}}, \gamma_{\mathrm{SR_b},p_1} \leq \gamma_{\mathrm{th}}\right) \Pr\left(\varphi_{\mathrm{R}_b\mathrm{E}_q,p_2} > \gamma_{\mathrm{th}}\right) \end{array} \right] \\
&= \mu_{\mathrm{E}_q,p_2} + \left(1-\mu_{\mathrm{E}_q,p_2}\right)\left(\theta_{\mathrm{R_b},p_2,p_1}\chi_{\mathrm{E},p_2} + \theta_{\mathrm{R}_b,p_2,\overline{p_1}}\tau_{\mathrm{E},p_2}\right).
\end{aligned} \tag{30}
$$

In (30), if E_q can correctly obtain p_2 at the first time slot (i.e., $\gamma_{\mathrm{SE}_q,p_2} > \gamma_{\mathrm{th}}$), it does not need to decode p_2 at the second time slot. Otherwise (i.e., $\gamma_{\mathrm{SE}_q,p_2} \leq \gamma_{\mathrm{th}}$), E_q correctly obtains p_2 in CASE 1 if $\gamma_{\mathrm{R}_b\mathrm{E}_q,p_2} > \gamma_{\mathrm{th}}$ or in CASE 2 if $\varphi_{\mathrm{R}_b\mathrm{E}_q,p_2} > \gamma_{\mathrm{th}}$. Then, substituting (13), (15), (18), (21), and (25) into (30), we obtain an exact closed-form expression of $\Lambda_{\mathrm{E}_q,p_2}$. Next, the probability that E_q correctly decodes one packet p_1 can be formulated as:

$$
\begin{aligned}
\Lambda_{\mathrm{E}_q,p_1} &= \Pr\left(\gamma_{\mathrm{SE}_q,p_2} > \gamma_{\mathrm{th}}, \gamma_{\mathrm{SE}_q,p_1} > \gamma_{\mathrm{th}}\right) \\
&+ \left[\begin{array}{l} \Pr\left(\gamma_{\mathrm{SE}_q,p_2} > \gamma_{\mathrm{th}}, \gamma_{\mathrm{SE}_q,p_1} \leq \gamma_{\mathrm{th}}\right) \\ \times \Pr\left(\gamma_{\mathrm{SR}_b,p_2} > \gamma_{\mathrm{th}}, \gamma_{\mathrm{SR}_b,p_1} > \gamma_{\mathrm{th}}\right) \\ \times \Pr\left(\gamma_{\mathrm{R}_b\mathrm{E}_q,p_1} > \gamma_{\mathrm{th}}\right) \end{array} \right] \\
&+ \left[\begin{array}{l} \Pr\left(\gamma_{\mathrm{SE}_q,p_2} \leq \gamma_{\mathrm{th}}, \gamma_{\mathrm{SE}_q,p_1} \leq \gamma_{\mathrm{th}}\right) \\ \times \Pr\left(\gamma_{\mathrm{SR}_b,p_2} > \gamma_{\mathrm{th}}, \gamma_{\mathrm{SR}_b,p_1} > \gamma_{\mathrm{th}}\right) \\ \times \Pr\left(\gamma_{\mathrm{R}_b\mathrm{E}_q,p_2} > \gamma_{\mathrm{th}}, \gamma_{\mathrm{R}_b\mathrm{E}_q,p_1} > \gamma_{\mathrm{th}}\right) \end{array} \right].
\end{aligned} \tag{31}
$$

In (31), if E_q correctly obtains p_1 from S (i.e., $\gamma_{\mathrm{SE}_q,p_2} > \gamma_{\mathrm{th}}$, $\gamma_{\mathrm{SE}_q,p_1} > \gamma_{\mathrm{th}}$), it does not need to decode p_1 any more. Next, if E_q correctly obtains p_2 and incorrectly p_1 (CASE 3.2) (i.e., $\gamma_{\mathrm{SE}_q,p_2} > \gamma_{\mathrm{th}}$, $\gamma_{\mathrm{SE}_q,p_1} \leq \gamma_{\mathrm{th}}$), then, in CASE 1, E_q uses SIC to remove p_2 and correctly decodes p_1 if $\gamma_{\mathrm{R}_b\mathrm{E}_q,p_1} > \gamma_{\mathrm{th}}$. If E_q cannot correctly obtain both p_2 and p_1 in the first time slot (i.e., $\gamma_{\mathrm{SE}_q,p_2} \leq \gamma_{\mathrm{th}}$ and $\gamma_{\mathrm{SE}_q,p_1} \leq \gamma_{\mathrm{th}}$), then, in CASE 1, E_q correctly decodes p_1 if $\gamma_{\mathrm{R}_b\mathrm{E}_q,p_2} > \gamma_{\mathrm{th}}$ and $\gamma_{\mathrm{R}_b\mathrm{E}_q,p_1} > \gamma_{\mathrm{th}}$.

In (31), the probability $\Pr(\gamma_{\mathrm{SE},p_2} < \gamma_{\mathrm{th}}, \gamma_{\mathrm{SE},p_1} < \gamma_{\mathrm{th}})$ can be calculated as

$$
\begin{aligned}
\mu_{\mathrm{E}_q,\overline{p_2},\overline{p_1}} &= \Pr\left(\gamma_{\mathrm{SE}_q,p_2} < \gamma_{\mathrm{th}}, \gamma_{\mathrm{SE}_q,p_1} < \gamma_{\mathrm{th}}\right) \\
&= F_{g_{\mathrm{SE}_q}}\left(\min\left(\rho_{\mathrm{th},1}, \rho_{\mathrm{th},2}\right)\right).
\end{aligned} \tag{32}
$$

Substituting (13), (16), (17), (22), (23) and (32) into (31), we obtain an exact closed-form formula of $\Lambda_{\mathrm{E}_q,p_1}$ as

$$
\begin{aligned}
\Lambda_{\mathrm{E}_q,p_1} &= \mu_{\mathrm{E}_q,p_2,p_1} + \mu_{\mathrm{E}_q,p_2,\overline{p_1}}\theta_{\mathrm{R}_b,p_2,p_1}\chi_{\mathrm{E},p_1} \\
&+ \mu_{\mathrm{E}_q,\overline{p_2},\overline{p_1}}\theta_{\mathrm{R}_b,p_2,p_1}\chi_{\mathrm{E},p_2,p_1}.
\end{aligned} \tag{33}
$$

Next, the IP of m_i $(i = 1, 2)$ at E_q can be calculated as

$$\mathrm{IP}_{\mathrm{E}_q,p_i} = \sum_{r=G_{\min}}^{H_{\max}} C_{H_{\max}}^{r} \left(\Lambda_{\mathrm{E}_q,p_i}\right)^{r} \left(1 - \Lambda_{\mathrm{E}_q,p_i}\right)^{H_{\max}-r}. \quad (34)$$

In (34), $(1 - \Lambda_{\mathrm{E_q},p_i})$ is the probability that E_q cannot decode one Fountain packet p_i correctly.

Then, m_i is intercepted if one of the eavesdroppers can intercept it. Therefore, the IP of m_i can be given as

$$\mathrm{IP}_i = 1 - \prod_{q=1}^{Q} \left(1 - \mathrm{IP}_{\mathrm{E}_q,p_i}\right) = 1 - \left(1 - \mathrm{IP}_{\mathrm{E}_q,p_i}\right)^{Q}. \quad (35)$$

In (35), $\prod_{q=1}^{Q} (1 - \mathrm{IP}_{E_q,p_i})$ is the probability that the data m_i is not intercepted by all the eavesdroppers.

Finally, the system IP is given as follows:

$$\mathrm{SIP} = 1 - (1 - \mathrm{IP}_1)(1 - \mathrm{IP}_2). \quad (36)$$

4. Simulation Results

Table 2. The system parameters

Parameter	Value	Description
a_{ST}	5	Fading severity parameter
b_{ST}	0.251	Multipath components
Ω_{ST}	0.279	Average power of LOS
λ_{RU}	0.01	Parameter of R-U_n channel
λ_{RV}	0.1	Parameter of R-V_m channel
λ_{RE}	50	Parameter of R-E_q channel
$P_{\mathrm{S}} = P_{\mathrm{R}} = P$	-	Transmit power of satellite and terrestrial relays
$\Delta = P/\sigma^2$	-	Transmit SNR
γ_{th}	1	Outage threshold
N	2	Number of users in Cluster 1
M	3	Number of users in Cluster 2
K	3	Number of relay stations
Q	2	Number of eavesdroppers

This section provides simulation results (**Sim**) to verify the theoretical analysis (**Theory**), and to illustrate the impact of parameters on the performance of the proposed scheme. Assume that the satellite links are subject to average shadowing. The main parameters used in the simulations are presented in Table 2.

Figs. 2–3 present OP and IP as a function of Δ [dB], respectively, when $G_{\min} = 8$ and $\alpha_1 = 0.25$. Fig. 2 presents that OP of both the cluster 1 (OP_1) and the cluster 2 (OP_2) decreases as Δ increases (since the transmit power of S and R increases). Next, OP_1 and OP_2 decrease with the increasing of $H_{\max}$. It is due to the fact that the users in two clusters have more

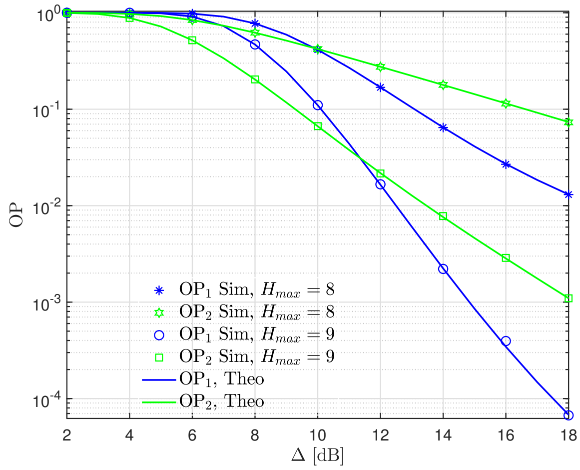

Figure 2. OP as a function of Δ [dB] when $G_{\min} = 8$, and $\alpha_1 = 0.25$.

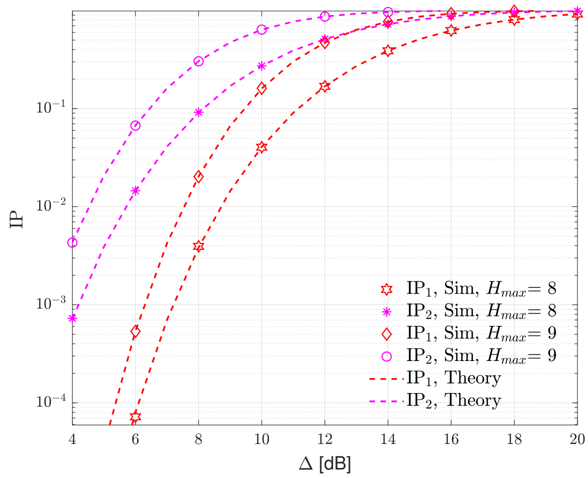

Figure 3. IP as a function of Δ [dB] when $G_{\min} = 8$, and $\alpha_1 = 0.25$.

opportunity to collect enough Fountain packets for the data recovery. Fig. 2 also shows that OP_1 is lower than OP_2 at high Δ values, and vice versa. In Fig. 3, it is observed that IP of both the data m_1 (IP_1) and the data m_2 (IP_2) increases as Δ and $H_{\max}$ increase. It is also seen from Fig. 3 that IP_2 is almost higher than IP_1. The results in Figs. 2–3 indicate that there exists a trade-off between OP and IP, with respect to Δ and $H_{\max}$. It is seen that the Sim and Theory results are in a good agreement, which validates the exactness of equations (28) and (35) in Section 3.

Figs. 4–5 present OP and IP as a function of the power allocation factor α_1, respectively, when $\Delta = 10$ [dB], $G_{\min} = 8$ and $H_{\max} = 9$. In Fig. 4, the number of terrestrial stations is set by $K = 1, 3, 5$. As we can see, OP_1 (OP_2) decreases (increases) as α_1 increases.

It is due to the fact that as α_1 increases, more (less) transmit power is allocated to the signals of the users in Cluster 1 (Cluster 2). Furthermore, both OP_1 and OP_2 decrease as increasing K. It is seen from Fig. 4 that there exists a gap between OP_1 and OP_2 that also changes with the increasing of α_1. For example, with $K = 5$, the gap between OP_1 and OP_2 is high when α_1 is very small or very high. In addition, the values of OP_1 and OP_2 are almost the same when α_1 is about 0.2. Therefore, the power allocation factor α_1 should be designed appropriately to obtain the performance fairness between two clusters (or the OP gap is as small as possible). In Fig. 5, we can see that IP_1 (IP_2) increases (decreases) as α_1 increases. As expected, both IP_1 and IP_2 increase as the number of the eavesdroppers increases.

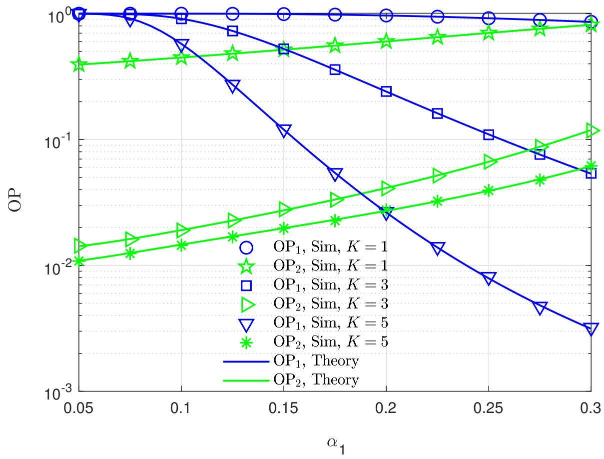

Figure 4. OP as a function of α_1 when $\Delta = 10$ dB, $G_{\min} = 8$ and $H_{\max} = 9$.

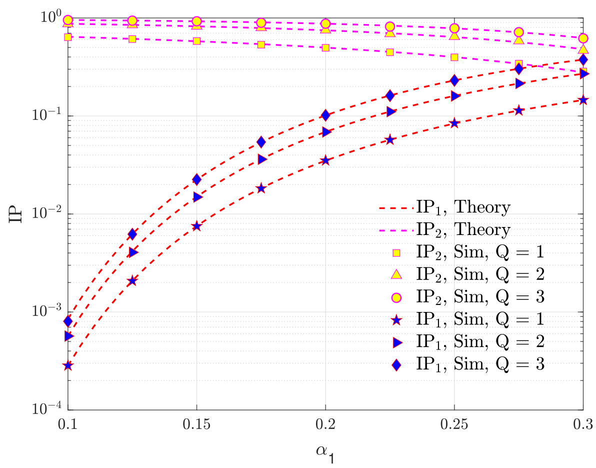

Figure 5. IP as a function of α_1 when $\Delta = 10$ dB, $G_{\min} = 8$, $H_{\max} = 9$.

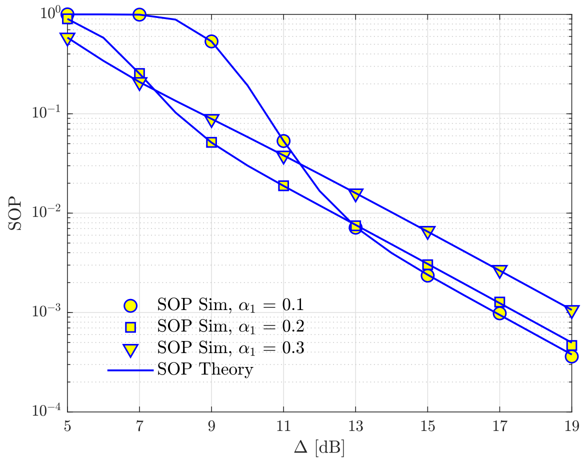

Figure 6. SOP as a function of Δ [dB] when $G_{\min} = 8$, $H_{\max} = 9$.

Figs. 6–7 present SOP and SIP as a function of Δ [dB], respectively, when $G_{\min} = 8$, $H_{\max} = 9$, $K = 8$, and $Q = 2$. In Fig. 6, we see that SOP increases when Δ increases (or the transmit power P increases). It is also seen from Fig. 6 that the value of α_1 significantly impacts on SOP. As we observe, at very low Δ values, SOP is the lowest with $\alpha_1 = 0.3$, and at high Δ values, SOP is the highest with $\alpha_1 = 0.1$. On the contrary to SOP, Fig. 7 presents that SIP increases with the increasing of Δ and the decreasing of α_1. Therefore, from Figs. 6–7, we can see that there also exists a trade-off between SOP and SIP. As expected, the Sim and Theory results in Figs. 6–7 match very well, which verifies the correctness of equations (29) and (36) in Section 3.

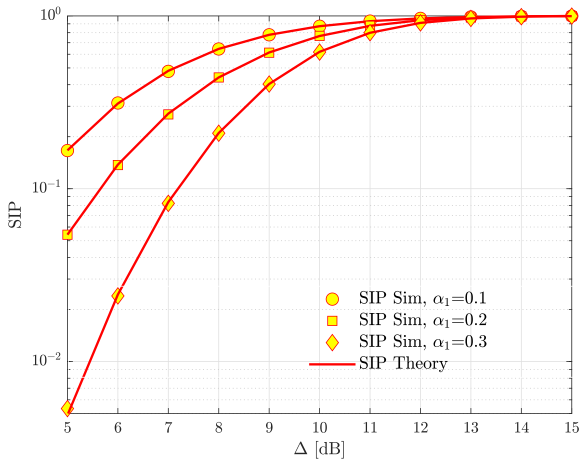

Figure 7. SOP as a function of Δ [dB] when $G_{\min} = 8$ and $H_{\max} = 9$.

Figs. 8–9 present SOP and SIP as a function of α_1, respectively, as $\Delta = 7.5$ [dB], $G_{\min} = 8$ and $H_{\max} =$

10. Similar to Figs. 4 and 6, α_1 significantly impacts on the SOP performance. Additionally, we can design the value of α_1 to obtain the best SOP performance. For example, with $K = 5$, the SOP performance is lowest with $\alpha_1 = 0.275$. Fig. 8 also shows that the SOP performance improves as the number of terrestrial stations (K) increases. In Fig. 9, we can observe that SIP decreases with the increasing of α_1. Moreover, the SIP performance degrades as the number of eavesdroppers increases. From Figs. 8–9, we can see that the security-reliability trade-off performance can be enhanced by increasing the number of terrestrial stations and appropriately designing the power allocation factors.

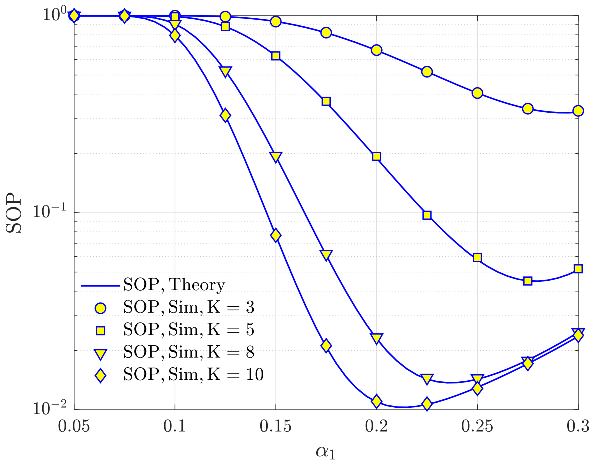

Figure 8. SOP as a function of α_1 when $\Delta = 7.5$ [dB], $G_{\min} = 8$, and $H_{\max} = 10$.

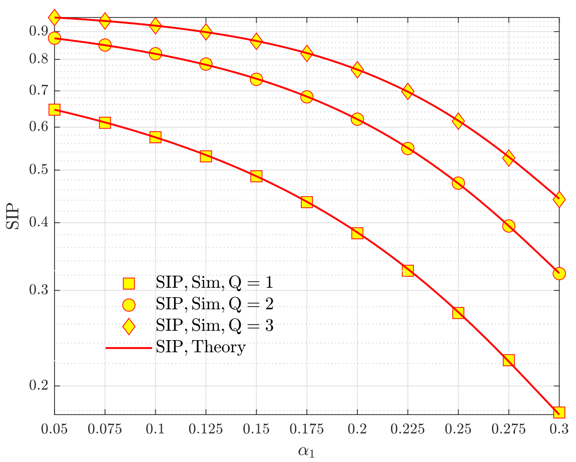

Figure 9. SIP as a function of α_1 when $\Delta = 7.5$ [dB], $G_{\min} = 8$, $H_{\max} = 10$, and $K = 5$.

5. Conclusion

This paper proposed and evaluated the performance of the proposed PLS-HSTRN scheme using FCs and NOMA via simulations and analysis. The results showed that there was a trade-off between reliability and security, following the transmit power of the transmitters and the number of transmission times of the satellite. To further enhance the OP, IP, SOP, and SIP performance as well as the SRT performance, the power allocation factors should be designed appropriately.

5.1. Acknowledgements

This work is funded by Vietnam National Foundation for Science and Technology Development (NAFOSTED) under grant number 102.04-2021.57.

References

[1] S. Chen, S. Sun, and S. Kang, "System integration of terrestrial mobile communication and satellite communication-the trends, challenges and key technologies in B5G and 6G," *China Communications*, vol. 17, pp. 156–171, Dec. 2020. DOI: 10.23919/JCC.2020.12.011.

[2] D. D. Tan, "Network coding design for reliable satellite communication services," *EAI Endorsed Transactions on Industrial Networks and Intelligent Systems*, vol. 6, p. e5, Dec. 2019. DOI:10.4108/eai.16-9-2019.160074.

[3] T. V. Nguyen, H. T. T. Pham, and N. T. Dang, "Joint adaptive modulation and power control scheme for energy efficient FSO-based non-terrestrial networks," *EAI Endorsed Transactions on Industrial Networks and Intelligent Systems*, vol. 12, Jan. 2024. DOI: https://doi.org/10.4108/eetinis.v12i1.7317.

[4] D. D. Tan, A. Masaracchia, B. Canberk, L. D. Nguyen, and T. Q. Duong, "Throughput maximization in RIS-assisted NOMA-THz communication network," *IEEE Open Journal of the Communications Society*, vol. 5, pp. 5706–5717, Oct. 2024. DOI: 10.1109/OJCOMS.2024.3454255.

[5] S. C. Lam and X. N. Tran, "Improving performance of the typical user in the indoor cooperative NOMA millimeter wave networks with presence of walls," *EAI Endorsed Transactions on Industrial Networks and Intelligent Systems*, vol. 11, p. e4, Apr. 2024. DOI:https://doi.org/10.4108/eetinis.v11i2.5156.

[6] A. S. Parihar, K. Singh, V. Bhatia, C.-P. Li, and T. Q. Duong, "Performance analysis of NOMA-enabled active RIS-aided MIMO heterogeneous IoT networks with integrated sensing and communication," *IEEE Internet of Things Journal*, vol. 11, pp. 28137–28152, Sep. 2024. DOI: 10.1109/JIOT.2024.3416951.

[7] T. T. Bui *et al.*, "Task offloading optimization for UAV-aided NOMA networks with coexistence of near-field and far-field communications," *IEEE Transactions on Green Communications and Networking*, 2025. DOI:10.1109/TGCN.2024.3417697.

[8] X. Yan, H. Xiao, C. X. Wang, and K. An, "Outage performance of NOMA-based hybrid satellite-terrestrial relay networks," *IEEE Wireless Communications Letters*, vol. 7, pp. 538–541, Aug. 2018. DOI: 10.1109/LWC.2018.2793916.

[9] S. Xie, B. Zhang, D. Guo, and B. Zhao, "Performance analysis and power allocation for NOMA-based hybrid satellite-terrestrial relay networks with imperfect channel state information," *IEEE Access*, vol. 7, pp. 136279–136289, Sep. 2019. DOI: 10.1109/ACCESS.2019.2942167.

[10] L. Han, W. P. Zhu, and M. Lin, "Outage of NOMA-based hybrid satellite-terrestrial multi-antenna DF relay networks," *IEEE Wireless Communications Letters*, vol. 10, pp. 1083–1087, May 2021. DOI: 10.1109/LWC.2021.3058005.

[11] V. Singh, V. Bankey, and P. K. Upadhyay, "Underlay cognitive hybrid satellite-terrestrial networks with cooperative-NOMA," in *2020 IEEE Wireless Communications and Networking Conference (WCNC)*, pp. 1–6, IEEE, May 2020. DOI: 10.1109/WCNC45663.2020.9120607.

[12] X. Zhang *et al.*, "Outage performance of NOMA-based cognitive hybrid satellite-terrestrial overlay networks by amplify-and-forward protocols," *IEEE Access*, vol. 7, pp. 85372–85381, Jun. 2019. DOI:10.1109/ACCESS.2019.2925314.

[13] B. Li, Z. Fei, C. Zhou, and Y. Zhang, "Physical-layer security in space information networks: A survey," *IEEE Internet of Things Journal*, vol. 7, pp. 33–52, Jan. 2020. DOI:10.1109/JIOT.2019.2943900.

[14] M. Elkashlan, L. Wang, T. Q. Duong, G. K. Karagiannidis, and A. Nallanathan, "On the security of cognitive radio networks," *IEEE Transactions on Vehicular Technology*, vol. 64, pp. 3790–3795, Aug. 2015. DOI: 10.1109/TVT.2014.2358624.

[15] F. Jameel, S. Wyne, G. Kaddoum, and T. Q. Duong, "A comprehensive survey on cooperative relaying and jamming strategies for physical layer security," *IEEE Communications Surveys & Tutorials*, vol. 21, pp. 2734–2771, Jul. 2019. DOI: 10.1109/COMST.2018.2865607.

[16] T. Q. Duong, J. Zhang, N. Yang, X. Zhou, and V. Sharma, Physical layer security for 6G networks. Institution of Engineering and Technology (IET), 2024. DOI: https://doi.org/10.1049/PBTE107E.

[17] K. Guo *et al.*, "Physical layer security for multiuser satellite communication systems with threshold-based scheduling scheme," *IEEE Transactions on Vehicular Technology*, vol. 69, pp. 5129–5141, May 2020. DOI: 10.1109/TVT.2020.2979496.

[18] K. Guo *et al.*, "Physical layer security for hybrid satellite terrestrial relay networks with joint relay selection and user scheduling," *IEEE Access*, vol. 6, pp. 55815–55827, Oct. 2018. DOI :10.1109/ACCESS.2018.2872718.

[19] Z. Lin *et al.*, "Refracting RIS-aided hybrid satellite-terrestrial relay networks: Joint beamforming design and optimization," *IEEE Transactions on Aerospace and Electronic Systems*, vol. 58, pp. 3717–3724, Aug. 2022. DOI:10.1109/TAES.2022.3155711.

[20] P. Q. Truong *et al.*, "Computation offloading and resource allocation optimization for mobile edge computing-aided UAV-RIS communications," *IEEE Access*, vol. 12, pp. 107971–107983, Aug. 2024. DOI:10.1109/ACCESS.2024.3435483.

[21] S. Pala, V. Singh, *et al.*, "Joint beamforming design and sensing in satellite and RIS-enhanced terrestrial networks: A federated learning approach," *IEEE Transactions on Cognitive Communications and Networking*, 2025. doi=10.1109/TCCN.2025.3526781.

[22] T. A. Lestari *et al.*, "Exploiting active STAR-RIS to enable URLLC in digitally-twinned Internet-of-Things networks," *IEEE Transactions on Communications*, 2025. DOI: 10.1109/TCOMM.2024.3471968.

[23] W. Cao, Y. Zou, Z. Yang, and J. Zhu, "Relay selection for improving physical-layer security in hybrid satellite-terrestrial relay networks," *IEEE Access*, vol. 6, pp. 65275–65285, Nov. 2018. DOI: 10.1109/ACCESS.2018.2877709.

[24] W. Cao, Y. Zou, Z. Yang, J. Zhu, and B. Li, "Security-reliability tradeoff analysis of hybrid satellite-terrestrial uplink communications with relay selection," *IEEE Systems Journal*, vol. 18, pp. 485–496, Mar. 2024. DOI: 10.1109/JSYST.2023.3344477.

[25] D. J. C. MacKay, "Fountain codes," *IEE Proceedings - Communications*, vol. 152, p. 1062, Dec. 2005.

[26] D. T. Hung, T. T. Duy, and D. Q. Trinh, "Security-reliability analysis of multi-hop LEACH protocol with fountain codes and cooperative jamming," *EAI Endorsed Transactions on Industrial Networks and Intelligent Systems*, vol. 6, p. e2, Jun. 2019. DOI: 10.4108/eai.28-3-2019.157120.

[27] T. L. Thanh *et al.*, "Broadcasting in cognitive radio networks: A fountain codes approach," *IEEE Transactions on Vehicular Technology*, vol. 71, pp. 11289–11294, Oct. 2022. doi=10.1109/TVT.2022.3188969.

[28] N. V. Toan *et al.*, "Outage performance of hybrid satellite-terrestrial relaying networks with rateless codes in co-channel interference environment," in *2023 International Conference on System Science and Engineering (ICSSE)*, pp. 468–473, IEEE, Jul. 2023. DOI:10.1109/ICSSE58758.2023.10227228.

[29] N. Q. Sang *et al.*, "On the security and reliability trade-off of the satellite terrestrial networks with fountain codes and friendly jamming," *EAI Endorsed Transactions on Industrial Networks and Intelligent Systems*, vol. 10, p. e3, Oct. 2023. DOI: https://doi.org/10.4108/eetinis.v10i4.4192.

[30] P. M. Quang, N. V. Toan, T. T. Duy, and P. N. Son, "Performance enhancement for rateless codes-aided hybrid satellite-terrestrial multi-user networks using NOMA and IRS with presence of multiple eavesdroppers," in *2024 9th International Conference on Consumer Electronics Asia (ICCE-Asia)*, pp. 1–4, IEEE, Jun. 2024. DOI: 10.1109/ICCE-Asia63397.2024.10773997.

[31] N. V. Toan, N. V. Hien, P. X. Minh, and P. N. Son, "Performance evaluation of hybrid satellite-terrestrial relaying broadcast networks using fountain codes and NOMA," in *2024 IEEE International Conference on Consumer Electronics-Asia (ICCE-Asia)*, pp. 1–4, IEEE, Jun. 2024. DOI:10.1109/ICCE-Asia63397.2024.10773917,.

[32] S. Lee, D. B. Da Costa, Q. T. Vien, T. Q. Duong, and R. T. de Sousa Jr, "Non-orthogonal multiple access schemes with partial relay selection," *IET*

Communications, vol. 11, pp. 846–854, Apr. 2017. DOI: https://doi.org/10.1049/iet-com.2016.0836.

[33] P. M. Nam *et al.*, "On the performance of the relay selection in multi-hop cluster-based wireless networks with multiple eavesdroppers under equally correlated Rayleigh fading," *EAI Endorsed Transactions on Industrial Networks and Intelligent Systems*, vol. 11, pp. 1–12, Jul. 2024. DOI: https://doi.org/10.4108/eetinis.v11i3.4728.

[34] W. Cao, Y. Zou, Z. Yang, and J. Zhu, "Relay selection for improving physical-layer security in hybrid satellite-terrestrial relay networks," *IEEE Access*, vol. 6, pp. 65275–65285, 2018. DOI:10.1109/ACCESS.2018.2877709.

[35] L. Han, W.-P. Zhu, and M. Lin, "Uplink outage performance of noma-based hybrid satellite-terrestrial relay networks over generalized inhomogeneous fading channels," *IEEE Transactions on Communications*, vol. 70, no. 4, pp. 2417–2434, 2022. DOI: 10.1109/TCOMM.2022.3148261.

[36] A.-T. Le, N.-D. X. Ha, D.-T. Do, S. Yadav, and B. M. Lee, "Enabling noma in overlay spectrum sharing in hybrid satellite-terrestrial systems," *IEEE Access*, vol. 9, pp. 56616–56629, 2021. DOI:10.1109/ACCESS.2021.3072362.

[37] D.-H. Ha, T. T. Duy, P. N. Son, T. Le-Tien, and M. Voznak, "Security-reliability trade-off analysis for rateless codes-based relaying protocols using noma, cooperative jamming and partial relay selection," *IEEE Access*, vol. 9, pp. 131087–131108, 2021. DOI:10.1109/ACCESS.2021.3114343.

[38] D. The Hung, T. Trung Duy, P. T. Tran, D. Quoc Trinh, and T. Hanh, "Performance comparison between fountain codes-based secure mimo protocols with and without using non-orthogonal multiple access," *Entropy*, vol. 21, no. 10, p. 982, 2019. DOI: https://doi.org/10.3390/e21100982.

[39] T. T. Duy, N. T. B. Le Chu Khan, N. T. Binh, and N. L. Nhat, "Intercept probability analysis of cooperative cognitive networks using fountain codes and cooperative jamming.," *EAI Endorsed Trans. Ind. Networks Intell. Syst.*, vol. 8, no. 26, p. e3, 2021. DOI: https://doi.org/10.4108/eai.26-1-2021.168229.

[40] N. T. Van, T. N. Do, V. N. Q. Bao, and B. An, "Performance analysis of wireless energy harvesting multihop cluster-based networks over nakagami- *m* fading channels," *IEEE Access*, vol. 6, pp. 3068–3084, 2018. DOI: 10.1109/ACCESS.2017.2787055.